

Ripple : Simplified Large-Scale Computation on Heterogeneous Architectures with Polymorphic Data Layout

Robert Clucas*, Philip Blakely, Nikolaos Nikiforakis

Maxwell Centre, Cavendish Laboratory, JJ Thomson Avenue, Cambridge, CB3 0HE

Abstract

GPUs are now used for a wide range of problems within HPC. However, making efficient use of the computational power available with multiple GPUs is challenging. The main challenges in achieving good performance are memory layout, affecting memory bandwidth, effective use of the memory spaces with a GPU, inter-GPU communication, and synchronization. We address these problems with the Ripple library, which provides a unified view of the computational space across multiple dimensions and multiple GPUs, allows polymorphic data layout, and provides a simple graph interface to describe an algorithm from which inter-GPU data transfers can be optimally scheduled. We describe the abstractions provided by Ripple to allow complex computations to be described simply, and to execute efficiently across many GPUs with minimal overhead. We show performance results for a number of examples, from particle motion to finite-volume methods and the eikonal equation, as well as showing good strong and weak scaling results across multiple GPUs.

Keywords: Parallel computing, GPU, High performance computing, Graph, Tensor, Heterogeneous architecture

1. Introduction

The heterogeneous nature of compute servers containing multiple many-core CPUs as well as a large number of accelerators—usually GPUs—makes it difficult to take full advantage of the available computational resources. Programming one domain (i.e. CPU or GPU) effectively requires expert knowledge of the respective hardware and associated tools, but is especially true for GPU implementations, where the programming model is significantly different from that required to program many-core CPU-based systems. It is also typically more difficult to extract high levels of performance from accelerators due to the difference in hardware design between CPUs and GPUs, which makes the performance of GPU code very dependent on register use, lack of indirection, and regular memory access patterns. These effects are magnified once multiple accelerators are present in a system due to cost of data transfer between them.

Most existing software frameworks separate the computational domains, or provide improvements in either programmer productivity or performance, but not both. Therefore, we identify two categories which need to be addressed to achieve good performance on systems with many CPU cores as well as multiple accelerators: fine-grained parallelism and coarse-grained parallelism.

Within fine-grained parallelism, there is the parallelisation of data and the execution of the computation on the data. These are

usually the kernels which run on the accelerators, or across the many CPU cores in the system. Achieving good performance in this area requires tuning the data layout, kernel execution sizes, and use of specific memory regions on the computational devices (i.e. cache and shared memory).

Coarse-grain parallelism involves the scheduling of kernels which execute on the computational resources, partitioning of work across the heterogeneous devices, and the reduction of latency when data must be transferred or shared between the different devices.

There is very little existing work which addresses both areas, and specifically all mentioned sections within each area, effectively. Here we present Ripple¹, a software library which addresses the above problems, providing an interface for specifying both coarse- and fine-grained parallelism, as well as providing the user with a simple means for configuring all aspects of parallelism to allow good performance to be achieved for their application with minimal effort, and with limited knowledge of GPUs or parallel and distributed systems. The major contributions of our work are the following:

- **Polymorphic data layout for user-defined types:** Users can specify data layouts for user-defined classes as a template parameter, which allows the class to be used as either Array-of-Struct (AoS, contiguous layout) or Struct-of-Array (SoA, strided layout). We provide interoperability of the layouts so that they can be used seamlessly throughout an application. This allows users to determine the best layout for the problem, and to use different data

*Corresponding author

Email addresses: rjc201@cam.ac.uk (Robert Clucas), pmb39@cam.ac.uk (Philip Blakely), nn10005@cam.ac.uk (Nikolaos Nikiforakis)

¹https://robclu.github.io/ripple_docs/

layouts for each part of an application or execution domain.

- **Specification of the memory space:** The user can specify which memory space should be used for each block of the data involved in a computational kernel (for example, shared or global memory on the GPU). Achieving good performance on GPUs requires testing all memory spaces and data layouts for a problem, which is cumbersome for large applications. We allow the memory space to be specified (in a single line) at the point of computation, allowing the same data to be used in different memory spaces for different parts of an algorithm.
- **N-dimensional tensor data type and iterators:** We provide an N-dimensional tensor data type and an iterator interface over the space. This removes the need for error-prone manual memory allocation and index computations. Further, padding cells can be specified for the tensor, required for many stencil-type operations, and allow these can be filled from neighbouring tensors where necessary.
- **Expressive graph model for the structure of a series of kernels:** Kernels, and the implicit and explicit dependencies between them, can be specified at a high level as a Directed Acyclic Graph (DAG). The memory and computational dependencies can then be determined by the library allowing optimisation of kernel-scheduling to minimise the overall latency of the computation.
- **Heterogeneous computation** Kernel-execution can be specified in a graph for execution on the CPU or GPU, enabling heterogeneous computation and making it possible to fully utilise the available computational power of both domains in a system.

While our library allows general computation to execute on heterogeneous nodes, our focus is on computations performed on multi-dimensional tensor-like data partitioned across multiple GPU accelerators. We take this approach due to modern GPUs providing significantly more computational performance than CPUs, and their ability to process regularly laid-out data efficiently. Despite their much higher theoretical computational throughput, attaining this on the GPU is more difficult than for the CPU, so simplifying programmer effort for better utilisation of GPU accelerators has the largest overall benefit—particularly for problems which require non-trivial data structures.

Ripple requires a compiler implementing the C++-17 standard and therefore supports Clang 9, 10, and 11, with CUDA [1] versions 9.0 through 11.2, as the compiler for both host and device code, or CUDA versions ≥ 11 with `nvcc` as the device compiler with GCC versions $\geq 9.3.0$ or Clang versions $\geq 9.0.0$ as the host compiler, since CUDA 11.0 provided the first `nvcc` compiler with C++-17 support for device code.

The remainder of the paper is structured as follows: In Section 2 we review existing work. Section 3 gives an overview of the abstractions in Ripple. These are described in more detail in

Section 4 where we describe the n-dimensional tensor data type, polymorphic data layout functionality, a simplified method for accessing elements in polymorphic data types, and the iterator abstraction which allows efficient accessing of tensor data in kernels. At a higher level, Section 5 outlines heterogeneous allocators in Ripple for improving the performance of workflows with dynamic memory requirements, the graph interface for computational workflow description, how constraints can be placed on kernel data access to specify data dependencies between kernels in a graph, and how to schedule work between the CPU and GPU computational domains. In Section 6 we describe how work is scheduled on either CPU or GPU as appropriate. Then, in Section 7 we provide benchmarks for the performance of the fine-grained aspects of our library, while Section 8 shows the scaling performance of the library across multiple computational devices. In Section 9 we discuss the main limitations of the library and directions of future work, and Section 10 summarises the whole work.

2. Related Work

While most related work falls into either the fine- or coarse-grained categories, SYCL [2] does provide features for both. The latest revision has support for kernels written in C++17, which can be executed on a number of backends, allowing a lot of flexibility for supported hardware. The framework also allows for kernels to be executed across multiple devices if available. However, a lot of the work has to be done manually by the user, such as the partitioning of data and transfer of data between execution devices. The main limitations of SYCL are a lack of support for CUDA devices as a backend, which likely results in less efficiency on CUDA supported devices as OpenCL does not provide all the features available in CUDA. Additionally, a number of the abstractions we provide to make programming simpler and more efficient in a multi-GPU context, such as polymorphic data layout, iterators, multi-dimensional tensors, and the graph interface which handles data transfer between devices, are not available in SYCL.

2.1. Fine-grained Parallelism

There are a number of existing frameworks which allow code to be parallelised by the compiler following programmer directives. Examples are OpenMP [3] and OpenACC [4]. They are simple to use, but are limited in the complexity of computation which they can parallelize effectively. OmpSs [5] extends OpenMP to allow heterogeneous computation, but still requires a large amount of work from the programmer and does not provide cross-GPU functionality. These perform very well at parallelising simple loops, but are not able to handle more complex computations. A good overview of the benefits and limitations of these types of programming models is provided by Lee and Vetter [6].

Kokkos [7] is a more sophisticated solution which has seen significant use, particularly in scientific applications. It provides data-layout flexibility for simple data-types (not user-defined), and high-level constructs for offloading computation

to one of the supported many-core backends. While the functionality is vast, and performance is very good relative to raw CUDA, the interface is quite involved, particularly for custom data structures. The main limitation of Kokkos is that it requires the programmer to manage inter-GPU communication and data transfer explicitly with another library, such as MPI, thus requiring a good knowledge of the underlying hardware and its API. Additionally, it does not provide an interface for shared memory use on the GPU or polymorphic data layout, which can both provide significant performance improvements for some applications, as we show later.

2.2. Coarse-grained Parallelism

Task based programming models have recently become popular due to their ability to specify complex computational workflows at a high level, and have them run efficiently in parallel. These are particularly suited to CPUs due to the dynamic and irregular nature of the tasks in the computational flow. Early works are StarPU [8], which provides a scheduling environment for tasks to run on heterogeneous architectures, exhibiting good performance. HPX [9] is similar, but is C++ standard conforming and allows task-based work to be executed on larger-scale heterogeneous architectures. It provides similar functionality to our graph interface for specifying a computational flow, but does not provide fine-grained data-space abstractions or polymorphic data-layout, which reduce development complexity and improve performance. A more recent work is Cpp-Taskflow v2 [10], which has seen significant use of late. The second version extends the original implementation to allow tasks to be executed heterogeneously on both the CPU and GPU, but does not provide any GPU based abstractions for data spaces or data transfer between GPUs.

While all of these works provide good abstractions for task-based parallelism, they offer limited support for the fine-grained parallelism which is required to take advantage of the throughput provided by GPU accelerators.

Once multiple accelerators are present in a system, most applications require data-transfer between the accelerators which contributes significantly to the overall computation time due to the bandwidth and latency of the memory system, resulting in under-utilization of the accelerators as they wait for data to process.

Work addressing these issues includes CuMAS [11], which looks at reducing the latency of data-transfer with respect to GPUs, but for the multi-application space, rather than within a single specific application. Bastem *et al.* [12] provide a framework for overlapping data transfers and compute on the GPU, however, the overall use is limited by the requirement for kernels to be written using OpenACC, which they show to produce sub-optimal performance compared to CUDA. Lastly, Daino [13] is a framework for hiding memory-transfer latency, but specifically for Adaptive Mesh Refinement, which limits its scope.

3. Abstractions

Modern computational environments contain multiple nodes which communicate via an interconnect. Ideally the system architecture would be abstracted by the programming interface, but this is challenging, especially when the data transfers create dependencies between operations on different devices in the system. Thus there is a separation into coarse- and fine-grained parallelism, for which we provide a number of abstractions to allow the programmer to maximise performance in both areas.

The data abstractions we provide are tensors, polymorphic data layout, accessors, and allocators, which target fine-grained parallelism, while the execution abstractions, which facilitate coarse-grained parallelism, are iterators and graphs. We describe these in more detail in the following sections.

4. Data Abstractions

Here we describe the abstractions that deal with data; generally improving fine-grained parallelism.

4.1. Tensors

In Ripple, a tensor is an abstraction over a multi-dimensional space. It contains a data type, which is stored for each point in the multi-dimensional space, and the dimensionality of the space, both provided at compile-time as template parameters. Data types can be scalar, such as `double`, `float`, `int`, etc. or user-defined. When the type is user-defined, the data-layout data can be specified as polymorphic, allowing the storage of the class data in the tensor to be SoA (elements are strided) or AoS (elements are contiguous), as described in Section 4.2, and shown in Figure 1. When initializing the tensor data, the layout is inferred from the data type, and the size of each dimension in the space is specified as a run-time parameter when the tensor is created, which can be resized if necessary.

Many operations require the use of data within a stencil. For example, an approximation of the first derivative of f using a forward difference in the x dimension at index u is

$$\Delta_x f_u = f_{u+1} - f_u \quad (1)$$

which requires access to the data point f_{u+1} . If f_u is at the boundary of the domain, the data at f_{u+1} is invalid, so padding data is required, which can be specified as a parameter when a tensor is created. Ripple provides a number of methods for loading the padding for common cases—such as first order and constant extrapolation. Padding becomes more complicated when the tensor data is strided or exists on multiple devices, potentially introducing a memory dependency in the DAG representing the computation, and Ripple simplifies the handling of the padding data in such cases. Through the graph interface, options are provided for the strictness of the dependency on operations which use or modify padding data, allowing the computational graph to be optimized to minimise the latency of memory operations as well as removing the need for the programmer to implement these themselves. These operations are described fully in Section 5.3.

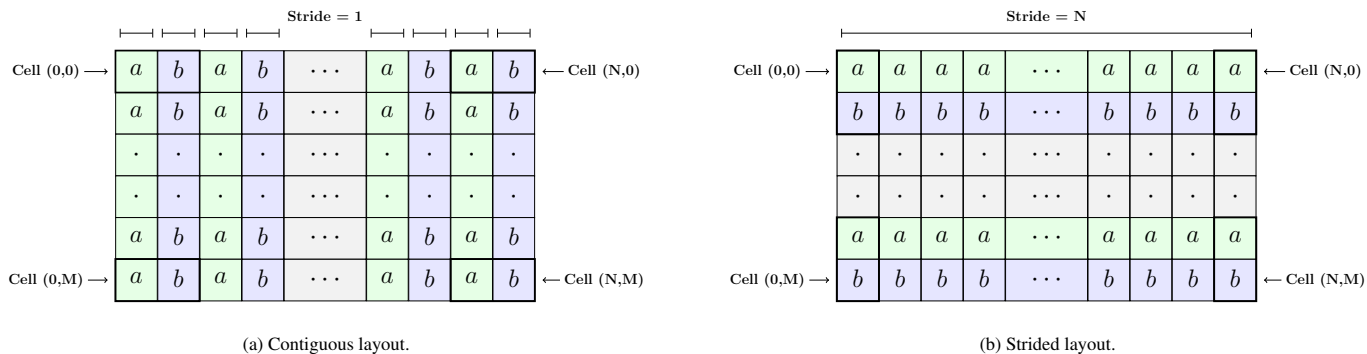


Figure 1: Illustration of strided and contiguous layouts for a struct with two components, p and p .

The tensor data can be partitioned across the system devices, and also within each device. An example is shown in Listing 1. This only requires changing a single parameter, making benchmarking straightforward. Partitioning across multiple dimensions results in smaller blocks in each of the partitioned dimensions. However, this requires data to be transferred between the devices if neighbour data is accessed, introducing dependencies in the DAG. We suggest partitioning across a single dimension for best performance. For multi-dimensional tensors, partitioning the higher dimensions is likely the best strategy because it results in a memory transfer of data which has a coalesced access pattern (i.e. accesses contiguously laid out data).

As shown in Listing 1, the tensor interface allows both the number of partitions per dimension, as well as the number of sub-partitions to be specified for each dimension. Sub-partitions exist on the same device so may introduce a memory dependency where one might not be necessary. However, they may also increase the overall opportunity for parallelism in an application, or create partition sizes which are suitable for both the CPU and GPU, leading to improved performance.

4.2. Polymorphic Data Layout

Tensor data layout is determined by the data type, which is always contiguous, unless the data type is user-defined and inherits from the `PolymorphicLayout` struct, which requires a template parameter to specify the type of layout. This allows user-defined types to have flexible data layout, and therefore the option to profile which layout is the best for different parts of an application. In Ripple, the layout of the class data can be defined as *contiguous* or *strided*. Contiguous data has the elements of the struct laid out contiguously in memory, while strided data is laid out with a stride equal to the size of the first dimension in the tensor. Internally, strided data stores an array of each of the components of the struct contiguously, with the component arrays being stored successively. These two layouts are shown in Figure 1.

Creating a polymorphic data layout requires a user-defined class to specify the types stored using the `StorageDescriptor` template class, which takes the layout and a list of types to be stored, similar to `std::tuple`. We provide a `Vector<T, Size>` class to specify that `Size`

elements of type `T` should be stored in a vector-like container. There are existing solutions which allow polymorphic layout within containers, but only for built-in types such as `double`, `float`, `int`, etc. Additionally, accessing the elements is done through an index, which does not provide the context that the name of a struct member does, and does not allow the polymorphic data to be used as both an object and within the tensor. Both of these limitations are significant in the development of large software projects. Ripple allows heterogeneous types to be stored in the tensor, and class-data to be accessed through the `StorageDescriptor` as if it were a `std::tuple`. The types must be defined through the `StorageDescriptor` interface rather than directly within in the class, and to inherit from the `PolymorphicLayout<T>` trait-class, allowing Ripple to determine that the user-defined type has a polymorphic memory layout with no runtime-overhead. The `StorageDescriptor` provides an alias for the actual storage type, and the elements can be accessed through the `get` template method which computes offsets at compile time. An example is shown in Listing 2 which defines a state class with `D` elements of type `T` and a `bool` indicating whether the state is valid. When used with a tensor, this will lay out the data based on the type provided as the `Layout` template parameter.

4.3. Accessors

For some use cases, it is more descriptive to define the members of a class as public, rather than as member functions which access the associated components from the storage, as shown in Listing 2. One such example is that of a vector class, with components for `x`, `y`, `z`, etc., which could be implemented with `x`, `y`, `z` as public members that can be accessed directly. However, if the storage is a contiguous array, they would have to be defined as public member functions for getting and setting the values, or would have to be stored as public members, which would require specialization for each number of elements.

We provide an `Accessor<ValueType, StorageType, Index>` abstraction to allow a given index in the storage to return a given value type, while still allowing the polymorphic layout flexibility. The accessor(s) can be used in a union with the storage type for a class to provide a more concise interface

```

/* Create a 2D tensor of doubles:
 * - 2 partitions per GPU in dimension 0 (x)
 * - 2 partitions per GPU in dimension 1 (x)
 * The resulting data sizes across the devices is:
 * (500, 500) | (500, 500)
 * -----
 * (500, 500) | (500, 500)
 */
constexpr size_t size_x = 1000;
constexpr size_t size_y = 1000;
Tensor<double, 2> t({2, 2}, size_x, size_y);

/* Create a 2D tensor of doubles:
 * - 2 partitions dimension 0 (x)
 * - 2 sub-partitions per partition in dimension 0 (x)
 * - 2 partitions per dimension 1(y)
 * - 2 sub-partitions per partition in dimension 1 (y)
 * The resulting data sizes across the devices is:
 * (250, 250) (250, 250) | (250, 250) (250, 250)
 * (250, 250) (250, 250) | (250, 250) (250, 250)
 * -----
 * (250, 250) (250, 250) | (250, 250) (250, 250)
 * (250, 250) (250, 250) | (250, 250) (250, 250)
 */
constexpr size_t size_x = 1000;
constexpr size_t size_y = 1000;
Tensor<double, 2> t({2, 2}, {2, 2}, size_x, size_y);

```

Listing 1 Tensor domain split example. Solid lines are device boundaries.

for data access. Additionally, nested unions can be used to overload the functionality of each of the storage elements, allowing access as x or r, depending on context. An example is shown in Listing 3 for a vector class. The advantage of the accessor implementation over a public member implementation is that the class data can be laid out as strided or as contiguous data when used with the tensor.

5. Execution abstractions

In this section we describe abstractions relating to the flow control; typically associated with coarse-grained parallelism.

5.1. Allocators

Often memory requirements are not known upfront, and therefore require memory to be allocated dynamically. However, this significantly reduces performance since `cudaMalloc` and `cudaFree` require synchronization to ensure that the memory being allocated or freed is not touched before or after the operation. These calls introduce significant points in the execution pipeline of an application where no work is being performed on either the CPU or the GPU. It is thus important to avoid dynamic allocation during a computation. For the Euler example presented in Section 8, dynamic allocations, even accounting for only 2% of the total memory requirement, caused performance reductions of up to 30%.

We therefore provide an allocator, `MultiarchAllocator`, which provides dynamic memory allocators for the CPU and the GPU via the `cpu_allocator()` and `gpu_allocator()` methods, respectively. For the CPU, we allocate a buffer of pinned host memory, since this is faster for transfer to the GPU and is required for asynchronous copies between the CPU and GPU. For the GPU we allocate a buffer with `cudaMalloc`, from

```

template <typename T, size_t D, typename Layout>
struct State {
public PolymorphicLayout<State<T, D, Layout>> {
// Declare storage for D elements of type T and a bool.
using Desc = StorageDescriptor<
Layout, Vector<T, D>, bool>;
using Storage = typename Desc::Storage;

// Normal access for vector:
// Gets the ith component from the vector
auto operator[](size_t i) -> T& {0
return storage.get<0>(i);
}

// Density is element 0 of type 0 from storage:
auto density() -> T& {
return storage.get<0, 0>();
}
// Pressure is element 1 of type 0 from storage:
auto pressure() -> T& {
return storage.get<0, 1>();
}
auto is_valid() const -> bool {
return storage.get<1>();
}

Storage storage;
};

// Specialization of the type for strided:
using State3d = State<double, 3, StridedView>;

```

Listing 2 Polymorphic layout example

which the allocator allocates. We use the same allocation strategy for the CPU and GPU allocators, which is to allocate linearly from the buffer. The CPU allocator has a buffer per thread, while the GPU allocator has a buffer per GPU, and both are thread safe to allow them to function correctly with the scheduler described in Section 6. Since the linear allocation strategy is relatively simple, we plan to extend the allocation strategy in future. For our use cases, however, the current implementation significantly improved overall performance in multiple applications. This was also the case for performing an out of place reduction across multiple devices, since the results buffers for the the reduction of the individual devices did not need to be allocated reducing the time for which the GPU was idle. We also provide constructors for the tensor data type which allow it to take a `MultiarchAllocator` from which it can allocate, for tensors requiring dynamic creation or resizing.

5.2. Iterators

When a callable is defined and operates on a tensor, its parameter type for each tensor is either an `IndexedIterator<T, Space>` or a `BlockIterator<T, Space>`, where T is the type of the tensor data and Space is the multi-dimensional space of the block within the tensor on which the iterator can iterate. The layout of the data iterated over is always the same as that of the tensor, and includes padding data if present. The iterator is automatically offset to the relevant cell in the tensor, avoiding the need for the user to have to perform any offsetting over padding data. The layout of the data is hidden by the iterator so that it can iterate over both contiguous and strided data.

```

template <typename T, size_t D, typename L>
class Vec : public PolymorphicLayout<Vec<T, D, L>> {
    using Desc = StorageDescriptor<L, Vector<T, D>>;
    using Storage = typename Desc::Storage;

    // Accessors types:
    using X = Accessor<T, Storage, 0>;
    using Y = Accessor<T, Storage, 1>;
    using Z = Accessor<T, Storage, 2>;
    using W = Accessor<T, Storage, 3>;

    union {
        Storage storage;
        X x; Y y; Z z; W w;
    };
};

// Usage
Vec<int, 3, ripple::ContiguousOwned> v;
v.x = 10, v.y = 20;

```

Listing 3 Vec implementation example using accessors

```

/* Creates a callable which takes an iterator, computes
 * the central difference in each dimension, and sums it.
 * We use auto for the iterator type for brevity.
 */
auto callable = [] ripple_host_device (const auto& it) {
    double diff_sum = 0.0;
    unrolled_for<iterator_traits_t<Iterator>::dims>(
        [&] (auto dim) {
            diff_sum += *it.offset(dim, 1)
                - *it.offset(dim, -1);
        });
};

```

Listing 4 Iterator offsetting in multiple dimensions

5.2.1. Indexed Iterator

The `IndexedIterator` carries with it indices which define the location of its block within the tensor, as well as its indices in the global iteration space, allowing the iterator to provide thread, block, and global indices and sizes. This allows the multi-dimensional space, partitioned across multiple devices, to appear as a single space. The iterator, however, can only iterate within a single block in the partitioned tensor space, due to the tensor data for different blocks potentially being on different devices.

This has an overhead per thread of 12 bytes per dimension in the tensor and iterator. However, benchmarks have shown the performance effect to be small, and the increase in ease of use of iterators compared to raw multi-dimensional indices is significant. The performance implications of the iterator framework are provided in Section 7. An additional benefit of the iterator is that the syntax for accessing data is consistent for different dimensions. Most frameworks overload `operator()` to enable indexing in multiple dimensions requiring separate specializations for each number of dimensions. While sometimes necessary, other operations differ only in the number of dimensions, thus, the iterator provides a compile time trait for the number of dimensions, and an `unrolled_for<dims>(operation)` method is available to unroll an operation for a number of dimensions as shown in Listing 4. We have benchmarked code which uses `unrolled_for` against a regular loop with a run-time value and have observed slightly better performance, and lower register usage on the GPU, in almost all cases.

```

Graph g(ExecutionKind::Cpu);
g.emplace([] { std::cout << "A\n"; });
g.then([] { std::cout << "B\n"; });
g.emplace(
    ExecutionKind::Gpu, /* Specify GPU execution. */
    make_node(
        [] (const char* s) { printf("%s", s); }, "C\n"),
    make_node(
        [] (const char* s) { printf("%s", s); }, "D\n"))
g.then([] { std::cout << "E\n"; });

```

Listing 5 Basic graph creation API

The iterator is similar to that in the standard C++ library, with extensions to support a multi-dimensional space. An iterator can be offset in a given dimension, as shown in Listing 4, and de-referencing provides access to the underlying offset data. Calls to the offset method can be chained to offset in multiple dimensions. When a callable is executed, a check is performed on the iterator's index against the the bounds of the multi-dimensional iteration space so that any out of range iterators do not execute the callable, ensuring that iterators only run on data valid within the tensor space.

5.2.2. Block Iterator

A `BlockIterator` is a lightweight version of the `IndexedIterator`, and used in more performance critical contexts. It iterates over a subspace of a tensor partition, and does not contain index information for the global space so cannot determine its global location. It can, however, provide the index with the subspace it can iterate over. A `BlockIterator` can be created over both statically and dynamically sized spaces. In the statically sized case, the size of the iterator is the size of a pointer, while for a dynamically sized space an additional four bytes are required per dimension to store the strides for iteration. An additional benefit of statically sized spaces is that the index computations are performed at compile time, as well as the determination of the amount of memory required for the space (shared memory on the GPU, or allocation from a pool on the CPU). In practice, these differences are minor compared to the computation time of kernels, and the `BlockIterator` over both static and dynamic spaces gives similar performance, which is improved compared to the `IndexedIterator` in contexts where memory is scarce, such as in shared memory. The interface for `BlockIterator` is a subset of the `IndexedIterator` interface, with the `IndexedIterator` providing additional functions which return information about the global iteration space, and traits to determine the type of an iterator.

5.3. Graphs

Graphs in Ripple allow a complete workflow to be described at a high level, from which the dependencies are determined when the graph is built. While the overhead of determining the graph-dependencies is minimal, we incur it at the time of graph creation because a graph is typically built once but executed many times. The graph is then submitted to an executor, which executes the nodes of the graph in parallel such that the dependencies are met. Operations are emplaced onto the graph,

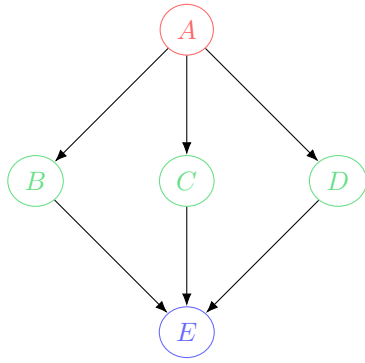


Figure 2: Graph structure for the code shown in Listing 5. Colours are used to illustrate nodes on the same level. Node A is the root node, on level 0. A, B, and C may execute in parallel, as soon as A completes, and E may execute once B, C, and D are all complete.

and can be divided into those on tensor and non-tensor types. In this context, a graph is a Directed Acyclic Graph (DAG), where nodes represent the computations (kernels) to be performed and edges represent the dependencies between the computations. We define a level in the graph to contain all nodes which have a dependency on a node in the previous level, with all nodes having no dependencies being the first level. Nodes on the same level may execute in parallel, as soon as their dependencies are met. The Graph constructor takes an argument for the default type of execution space, which can also be overridden for each operation, as either `ExecutionKind::Cpu` or `ExecutionKind::Gpu`. A simple example of the levels in the graph is illustrated in Figure 2

5.3.1. Nodes

The nodes in a graph are defined using a `Node` which stores the callable defining the node operation, as well as any arguments which are required to invoke the callable. To allow callables with any signature, type erasure is used to store a generic executor in the node, which is different from most existing solutions that require callables to have a specific signature. In addition to the callable object, the node stores information to allow it to be accessed and modified after the graph has been created.

5.3.2. Operations on non-tensor types

In some task-based models, nodes are added to the graph and then the dependencies are specified. However, we take a different approach, where the graph is defined more explicitly and concisely. We also provide functionality for modifying dependencies between individual nodes after graph creation by allowing nodes to be searched for by the node name. The operations which add non-tensor based operations to a graph are `emplace()` and `then()`.

Emplace. `Emplace` adds a node onto the graph, with the dependencies of the node being any nodes in the previous level. To allow multiple nodes to be placed in the same level (such that they execute in parallel), `emplace` can be called multiple times,

```

Tensor<double, 1> x({1}, {4}, size);

Graph g(ExecutionKind::Cpu)
g.emplace([] { std::cout << "A\n"; }, )
.emplace([] { std::cout << "B\n"; }, )
.then_split(
  ExecutionKind::Gpu,
  [] ripple_host_device (auto& it) {
    *it = 1.0;
  }, x);

```

Listing 6 `Emplace then split` example

or by using the `make_node()` function which allows multiple callables to be added through a single call to `emplace()`. Listing 5 shows example usage for the `emplace()` interface.

Then. The `then()` method creates a dependency in the graph, by indicating that the work defined for a new node must be run after previously emplaced nodes. The new node is added as a successor of all nodes in the previous level, and will only be run after *all* its dependents have finished. Listing 5 shows the code for creating a graph and Figure 2 shows the structure of the corresponding graph.

5.3.3. Operations on tensor types

For tensor operations, data may be spread across multiple devices, and therefore a node which defines its operation on a tensor will, in most cases, have the partitions of the tensor execute in parallel. To reduce overall latency, the kernel must ideally be submitted asynchronously to the device on which the partition of the tensor data exists, so that it can begin execution as soon as all dependencies are met. If a single node were to define the operation on the tensor then the submission of the kernel to the multiple devices would be sequential (since if there is a single node running on a single thread, but multiple kernels are required to be submitted for each partition, the submissions must be serial). To avoid this, when a kernel is emplaced onto a graph which operates on a tensor, a node is automatically created for each partition in the tensor, with each node being on the same level. This allows the kernel associated with each node to be submitted to the device in parallel, using any number of the available GPU cores in the system. This is more challenging to achieve when the tensor has padding, since memory transfer nodes are required to copy the padding data from another device, which may need to complete before the node with the kernel is executed. We provide utilities to allow the user to achieve as much parallelism as possible by allowing different requirements for the padding data transfer to be specified, described in detail in Section 5.4. For adding nodes which operate on tensors, the `split()` and `then_split()` methods are provided, so named to indicate that the operation is split into multiple nodes for each of the tensor partitions.

Split. On nodes emplaced for computations on tensor data, `split()` has the same effect as `emplace()` in that it will emplace nodes onto the graph at the current level, with each of the nodes having a dependency on the nodes in the previous level. If the tensor does not require any padding, `split()` creates a

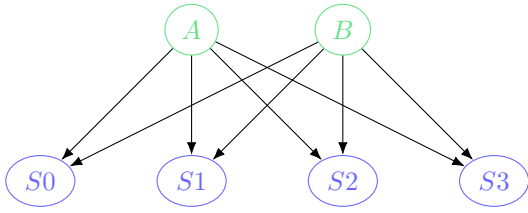


Figure 3: Graph structure for the code shown in Listing 6. Nodes S0-3 represent the nodes generated for the split operation.

node per tensor-partition, and each of these nodes may execute concurrently. Listing 7 illustrates code which defines a graph to perform the well-known saxpy example using four GPUs.

Then Split. The `then_split()` method allows dependencies to be created between operations on previously emplaced nodes and the nodes generated by subsequently splitting a tensor. The method specifies that the new operation on each partition of the split tensor must happen after any previous operations in the graph. If the previous operation was a `split()` or `then_split()` operation, then dependencies are only added between nodes associated with the *same* partitions in the tensor. This reduces the overall required connectivity of the resulting graph by reducing the number of synchronization points. If a `then_split()` operation is added after a non-tensor operation, then each node generated depends on *all* operations in the previous level. This is illustrated in Figure 3 which shows the graph generated by Listing 6.

Reduction. The `reduce()` and `then_reduce()` operations operate specifically on tensors, and reduce the data in the tensor into a `ReductionResult<T>` type which stores the result of the reduction as well as a flag indicating whether the reduction is complete. The flag is required because for tensors where data is spread across multiple devices the reduction for each partition of the tensor may happen asynchronously. This design allows each partition to perform the reduction of its data as soon as its dependencies are met, so that the entire reduction across multiple devices finishes sooner than if the reduction was started once *all* nodes in the previous level were complete. It also allows subsequent nodes associated with the partition to continue if they do not have any dependency on the result of the reduction. Similarly to `then_split()`, for nodes in the previous level that are associated with the *same* partitions on which the reduction will be performed, there is only a dependency be-

```
Tensor<double, 1> x({4}, size);
Tensor<double, 1> y({4}, size);

Graph g(ExecutionKind::Gpu);
g.split(
  [] ripple_host_device (
    auto& x_it, auto& y_it, double a) {
      *y_it = a * (*x_it) + (*y_it);
    },
  x, y, 4.0);
```

Listing 7 Basic split SAXPY example

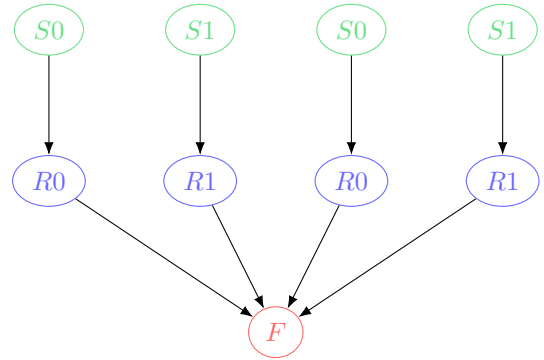


Figure 4: Graph structure for the code shown in Listing 8. Nodes S0-3 represent the nodes generated for the split operation, R0-3 the reduction operation, and F the operation which sets the reduction as complete. The dependencies allow, for example, for the possibility that R0 completes before S1 ends, depending on the dependencies of S0, if this graph were part of a larger graph.

tween the nodes associated with the same partitions, and not between the node performing the reduction and all other nodes in the previous level. Listing 8 shows an example for setting each value in a tensor and then performing a reduction sum, while the corresponding graph is shown in Figure 4. The operation for the reduction on the quarter of the domain represented by R0 in the graph depends only on the split operation S0 which operates on the same data, thus R0 can start as soon as S0 finishes, increasing overall parallelism. Additionally, the reduction is performed in shared memory on the GPU, which improves performance and only reads the tensor data from global memory, so there is no write dependency in subsequent operations, allowing other operations on the partitions to be added to the graph at the same level.

5.3.4. Synchronization

For larger graphs, some paths may progress more quickly than others, which may then need to be synchronized. To allow for all pending nodes to complete before any partition continues, the `sync()` function, with the same signature as `emplace()` and `split()`, can be used to emplace a node onto the graph which synchronizes all work from both domains, and then executes the callable for the `sync()` node.

```
Tensor<double, 1> x({4}, size);
auto result = make_reduction_result<double>(0.0);

Graph g(ExecutionKind::Gpu);
g.split(
  [] ripple_host_device (auto& it) {
    *it = 1.0;
  },
  x)
  .then_reduce(x, result, SumReducer());

// value = size
auto value = result.value();
```

Listing 8 Split then reduce


```

Tensor<double, 1> x({4}, size);
auto result = make_reduction_result<double>(0.0);

Graph init(ExecutionKind::Gpu);
Graph map_reduce(ExecutionKind::Gpu);
init.split(
  [] ripple_host_device (auto& it) {
    *it = 4.0;
  },
  x);

map_reduce
  .split([] (auto& it) { *it -= 1.0;})
  .then_reduce(x, result, SumReducer())
  .conditional([&result] {
    return result.value_and_reset() != 0.0;
  });

init.then(map_reduce);

```

Listing 9 Conditional map reduce with initialization

5.3.5. Subgraphs

To enable better separation of code, and overall flexibility in the graph creation API, we allow graphs to be added using the `emplace()` and `then()` operations, which adds the graph passed to the operation as a subgraph in the current graph, which will either execute in parallel with the nodes in the last level (for `emplace()`) or after the nodes in the last level (for `then()`). For complex graphs, this allows each of the subgraphs to be implemented separately, and then to be combined in a final step which defines the connectivity between the subgraphs.

To ensure that the resulting graphs are correct, the nodes in the last level of the graph onto which the subgraph is emplaced need to be connected to the nodes in the first level of the subgraph. For nodes on non-tensor types the process is simple since each node in the last level of the graph is connected to each node in the first level of the subgraph. However, as mentioned in Section 5.3.3, when the nodes in the levels operate on the same tensor partition then the node in the subgraph should only be connected to the node which corresponds to the same partition in the tensor, as well as any other non-tensor nodes in the previous level. If this is not the case, the operations on the tensor partition will wait longer than necessary due to an unnecessary dependency between the node and another tensor node which operates on a different partition.

5.3.6. Conditional execution

There is a trade-off between static and dynamic specification of a graph; if a graph is specified statically then compile-time optimizations can reduce its complexity so that the execution is more efficient, however, for most real-world applications, graphs likely need some form of dynamic behaviour at runtime. We provide dynamic behaviour through conditional operations that can be emplaced onto a graph, which determine whether or not the graph should be executed. A conditional node takes a predicate which returns `true` if the graph should execute, and `false` otherwise. Along with the subgraph functionality described in Section 5.3.5, this allows graphs of arbitrary complexity to be created which have completely dynamic runtime behaviour. The expressiveness of this functionality can be seen

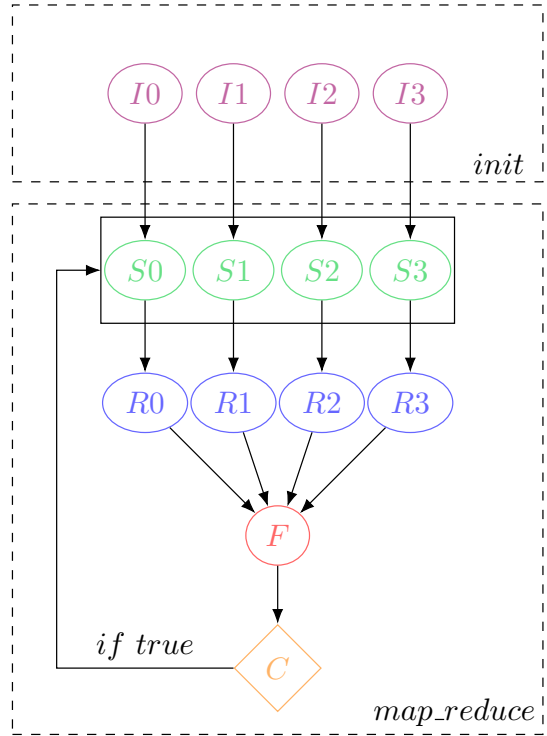


Figure 5: Graph structure for the code shown in Listing 9, indicating both graphs from the code listing, and the flow of control.

by combining the `split()` and `then_reduce()` operations on tensor data to provide a simple implementation of the MapReduce [14] framework. An example is shown in Listing 9 and the corresponding graph in Figure 5.

5.4. Tensor Data Dependencies

As described in Section 5.3, when nodes are added to the graph for tensor operations it is important to reduce the connectivity of the resulting graph. This allows operations on independent partitions of the tensor to begin execution as soon as possible, reducing synchronization during execution of the graph. The complexity of the graph, however, depends on how the kernel modifies the partition data associated with a node—whether the operation on the data requires concurrent or exclusive access and whether the tensor has padding accessed by the kernel.

The simplest case is a tensor operation requiring no padding, since it cannot require data from neighbouring partitions. This does not cause any ordering dependency between the node and any subsequent nodes which operate on the same data. Thus, when a tensor is passed to one of the methods for emplacing nodes onto the graph we assume this is how the tensor is accessed. For any other type of access, one of the methods for specifying the access requirement when the operation uses padding must be used, which ensures that the correct dependencies are added to the graph to avoid race conditions.

5.4.1. Concurrent access with padding

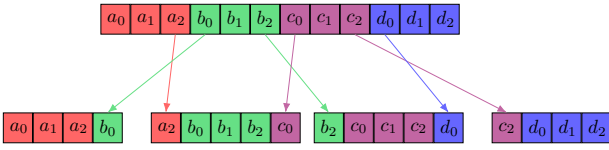


Figure 6: One-dimensional tensor data. Colours for data represent that data resides on the same device, colours for edges represent the device which performs the operation to move data along the edge.

When the tensor partition data can be accessed concurrently (i.e. there is no write to data which is used by a kernel on another partition) by a kernel and the access *will* use the padding data, then the `concurrent_padded_access()` modifier needs to be used when the kernel is emplaced onto the graph. Consider the one-dimensional tensor data in Figure 6, where the data is split across four devices and that the operation to be performed is the difference computation in Listing 10. The figure illustrates the padding which needs to be copied from neighbouring devices before the difference computation—which accesses the padding—can begin. Using the `concurrent_padded_access()` modifier, as shown in Listing 10, results in the associated graph shown in Figure 7. An additional node is inserted for padding data transfer operation from a partition to a neighbour partition, which ensures that the subsequent nodes can run concurrently as soon as their padding operations are complete. The padding operations *from* a node (Figure 7 (x_p)) can happen on different streams than the kernels for *the same* node (x_s) and, if the GPU supports it, can overlap in time. For example, in Figure 7, the operation a_p could happen in parallel with a_s , since the data copied by a_p is not modified in a_s . For the one-dimensional case, the highest padding cost is two copies (nodes b_{p1}, b_{p2}, c_{p1} and c_{p2} in Figure 7), however, for higher dimensional data the num-

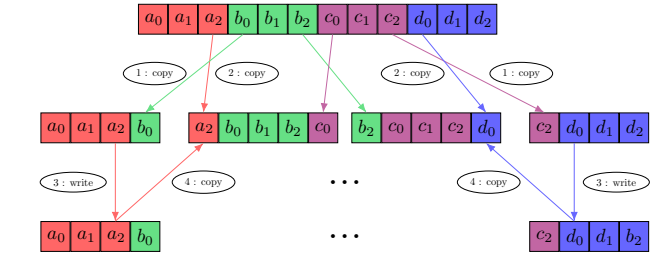


Figure 8: One-dimensional tensor data which shows a sequence where a potential race condition occurs between operations 2 and 3, which may result in the padding data a_2 being the updated value. Exclusive padded access, results in a graph which ensures that operation 2 *happens before* operation 3, removing the race condition so that the transferred a_2 is the original value.

ber of copies is significantly more if the data is split across all dimensions (8 for two dimensions, and 26 for three dimensions). While splitting data across fewer dimensions results in a lower number of data transfers, the best partitioning strategy is problem-dependent, hence why we make it easy for the user to specify.

5.4.2. Exclusive access with padding

When the tensor partition data needs to be accessed exclusively (i.e. there is a write to data which is required by a kernel on another partition) by the kernel for the node, and the kernel *will* use padding data, then the `exclusive_padded_access()` modifier needs to be used when the operation is emplaced onto the graph, as the resulting graph requires additional connections to prevent a race condition between data write-access in the kernel and the memory transfer operation of the same data to a neighbour which requires reading it for padding. This is illustrated in Figure 8 for the graph in Figure 7. Since all the operations to copy the padding data for the leftmost partition can execute in parallel, it is possible that the copy (operation 1)

```
Tensor<double, 1> x({4}, padding, size);
Tensor<double, 1> y({4}, size);

auto callable =
  [] ripple_host_device (auto&& in, auto&& out) {
    *out = *in.offset(ripple::dim_x, 1)
          - *in.offset(ripple::dim_x, -1);
  };

graph.split(
  callable, ripple::concurrent_padded_access(x), y);
```

Listing 10 Double buffered concurrent read example

```
Tensor<double, 1> x({4}, padding, size);

auto callable =
  [] ripple_host_device (auto&& in_out) {
    *in_out = *in_out.offset(ripple::dim_x, 1)
             - *in_out.offset(ripple::dim_x, -1);
  };

graph.split(
  callable, ripple::exclusive_padded_access(x));
```

Listing 11 Single data exclusive write example

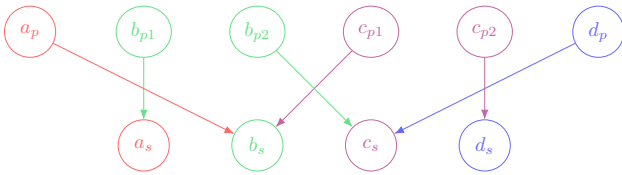


Figure 7: Graph for transferring concurrently accessed data with padding. Edge colours correspond to the data movement in Figure 6, where subscripts p and s correspond to the padding and split operations, respectively. Nodes of the same colour in different levels can execute concurrently.

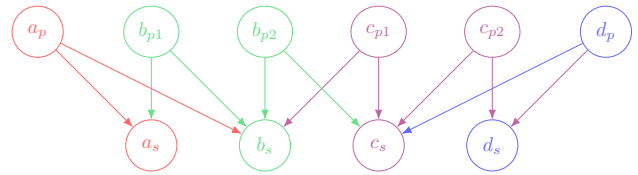


Figure 9: Graph for a one dimensional tensor which requires padding and where the subsequent operations write to the data, where subscripts p and s correspond to the padding and split operations, respectively. Nodes of the same colour in different levels cannot execute concurrently.

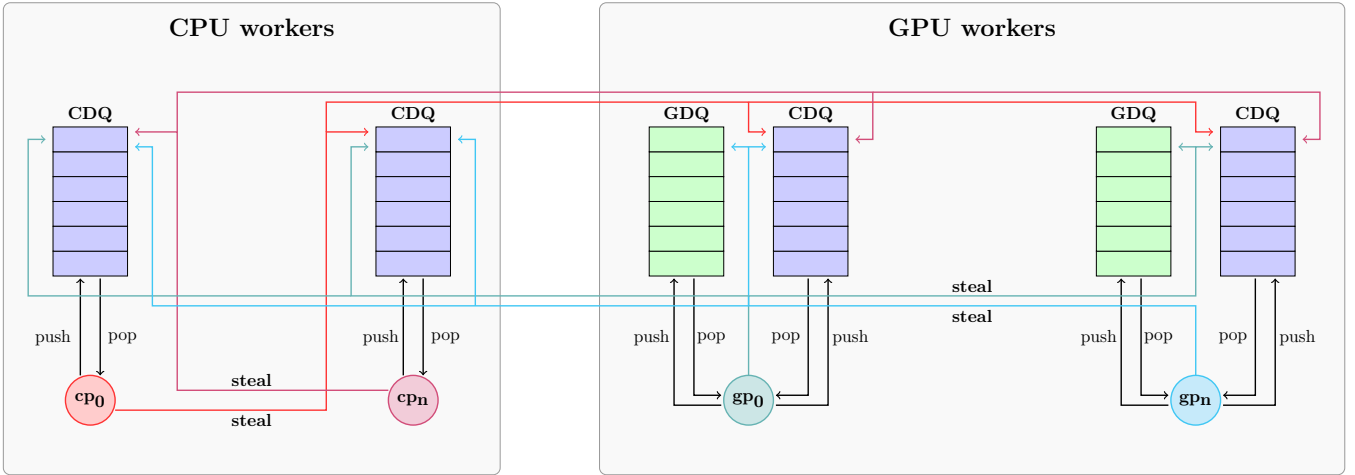


Figure 10: Design of our heterogeneous scheduler. coloured paths illustrate the possibility for a worker to steal from the queue to which the path leads.

for its padding completes before the copy (operation 2) for the second leftmost partition’s padding begins. Additionally, since for the graph in Figure 7 the split kernel and the data transfers for the same partition can happen concurrently, if dependencies for a write operation are not added in Figure 7, then there will be a race between operations 2 and 3 in Figure 8. This race happens for all the padding data, as illustrated by the rightmost data in Figure 8. To avoid this, the `exclusive_padded_access()` modifier specifies that a kernel will use padding data and requires exclusive access, allowing the library to include the required dependencies in the graph, as shown in Figure 9. The split operations on the second level, in addition to the dependencies of the padding operations from their neighbours, have dependencies on the padding operations to their neighbours. Such access is usually required when there is only a single instance of the data, which is updated within a kernel, as in Listing 11.

5.4.3. Shared access

We also provide access specifiers which create and copy the tensor data into shared memory, which can improve performance for some kernels. When the data has no padding, the `in_shared()` specifier can be

used, while for data which additionally requires padding, the `exclusive_padded_access_in_shared()` and `concurrent_padded_access_in_shared()` modifiers can be used to create these dependencies.

6. Scheduling

For scheduling, we use a modified form of the well-known work stealing algorithm. We provide an overview of the algorithm, and our extensions of the algorithm to multiple domains of execution—CPUs and GPUs.

6.1. Work Stealing

Work stealing is a common pattern for task-based parallelism and has been used successfully in [15, 16, 10]. A group of worker threads is spawned, each with its own queue of work from which tasks can be executed. When a thread’s queue becomes empty, it *steals* work from the queues of other worker threads [17, 18]. Once a worker thread completes execution of a task it looks to the successor of the completed task as the next candidate for execution, which can be executed if all the dependencies of the task are met [19]. The pool of worker threads

Algorithm 1 Worker thread main loop

Input: s : worker state
Input: t : worker thread

```

1: while (! $s$ .must_shutdown()) do
2:   if ( $s$ .paused()) then
3:      $s$ .suspend()
4:     continue
5:   end if
6:   if (execute_work( $s$ ,  $s$ .main_priority())) then
7:     continue
8:   end if
9:   execute_work( $s$ ,  $s$ .secondary_priority())
10: end while

```

Algorithm 2 execute_work(s , q)

Input: s : worker state
Input: q : queue type
Output: bool : if execution succeeded

```

1:  $node \leftarrow s$ .pop( $q$ )
2: if ( $node$ ) then
3:   if ( $node$ .try_execute()) then
4:      $s$ .increment_processed_nodes()
5:     return true
6:   end if
7:    $s$ .push( $node$ ,  $q$ )
8: end if
9: return steal( $s$ ,  $q$ )

```

Algorithm 3 `try_execute()`

Require: `n` : node to execute**Output:** `bool` : if execution succeeded

```
1: if (n.dependents.load()  $\neq$  0) then
2:   return false
3: end if
4: n.dependents  $\leftarrow$  n.initial_dependents
5: n.execute()
6: for each s in n.successors do
7:   s.dependents.fetch_sub(1)
8: end for
9: return true
```

continues to execute until all queues are empty, or the program terminates.

Most existing research on work stealing has focused on a single domain, which has primarily been the CPU in the context of large task-based systems which utilise hundreds to thousands of CPU cores. For heterogeneous domains, however, there is little work on using work stealing to achieve good parallel efficiency across domains. In such a context, worker threads could submit tasks for execution on either the CPU or the GPU, and the scheduling algorithm needs to ensure that the dependencies in the graph are met for the execution of both domains, while still being efficient. The most recent work for heterogeneous domains is that of [10]. However, their work focuses on the execution of large graphs on the CPU. While it does allow nodes to contain GPU work, it does not have knowledge of how data is accessed by kernels, and therefore cannot allow for determining data dependencies for GPU-based workflows, instead requiring that the user write all GPU code within the graph nodes. We follow their heterogeneous scheduler approach, but modify it to better support our higher-level GPU abstractions to allow good performance for GPU-based workflows.

6.2. Design

We use the general work stealing idea, with a pool of worker threads, however, we additionally give each worker thread a domain priority for the type of work it primarily schedules—as either CPU or GPU. The worker threads in the algorithm are adaptive, sleeping when there is not enough work for all threads in the domain, and waking when the workload increases, which is determined when nodes are scheduled for execution. Each worker thread stores state information to facilitate its suspension: the domain priority, the number of processed nodes, and the queue of nodes. The main loop for the worker threads in our scheduler is shown in Algorithm 1.

By default, we set the number of threads with GPU priority (GPUP) to be one more than the number of physical GPUs in the system, and the number of threads with CPU priority (CPUP) to be the number of remaining physical CPU cores in the system. In all benchmarks, using both more or less GPUP threads than this reduced performance due to either requiring more CUDA context switching and stream synchronization than necessary, when more threads were used, or too little parallelism, when fewer were used.

Algorithm 4 `steal(s, q)`

Input: `s` : worker state**Input:** `q` : queue type**Output:** `bool` : if execution succeeded

```
1: steal_id  $\leftarrow$  s.thread_id
2: for (i  $\in$  [0, s.steal_attempts]) do
3:   steal_id  $\leftarrow$  s.get_steal_id(s.steal_strategy)
4:   if (steal_id  $==$  s.thread_id) then
5:     continue
6:   end if
7:   node  $\leftarrow$  thread_states[steal_id].steal(q)
8:   if (node) then
9:     if (node.try_execute()) then
10:      s.increment_processed_nodes()
11:      return true
12:     end if
13:     s.push(node, q)
14:   end if
15: end for
16: return false
```

We must ensure that when multiple workers try to steal the same task from the same queue, it is only possible for *a single worker* to gain access to the task. Thus the main data structure for the scheduler is a lock-free implementation of a work stealing deque [20, 21], where the thread to which the queue belongs can push and pop from one end, while other threads can steal from the other end. GPUP threads have queues for both CPU (CDQ) and GPU (GDQ) work, and can push and pop onto either of their own queues (prioritising GDQs) or steal from the GDQ or CDQs (again prioritising the GDQs) of any other threads. CPUP threads, however, have only a single work stealing deque (CDQ) and can only push and pop from it, but can steal from any other CDQ, regardless of the domain priority of the thread to which the queue belongs. This allows all CPU cores to perform multi-threaded CPU work, but only a subset to perform submission and synchronization of GPU work, allowing an increase in the level of CPU parallelism when some GPU kernels are significantly longer executing than other CPU kernels.

In the work stealing deque for a worker thread, we encapsulate the work to be executed by the executor in a Node class—which represents a node in a graph to be executed—and store the nodes in the deque. The node contains information about its connectivity in the graph, via an atomic counter which stores the number of dependents, and a pointer to its successor, whose dependents counter needs to be decremented when the node completes its work, allowing the graph dependencies to be maintained. Within the `execute_work` function of Algorithm 1, a worker pops a node off one of its queues, tries to execute it, and then either exits, upon success, or tries to steal from another queue. This is shown in Algorithm 2, while the algorithm for attempting to execute a node’s work is shown in Algorithm 3. On line 5 of Algorithm 3 we restore the initial dependency count of the node before it finishes executing, which

Name	AWS p3.2xlarge	AWS p3.4xlarge	AWS p3.8xlarge
OS		Centos 7	
CPU		Intel Xeon E5-2686 v4	
CPU Frequency		2.3 GHz	
GPU		NVIDIA V100-SXM2	
GPU Architecture		Volta (sm 7.0)	
CUDA Cores		5120	
GPU Frequency		1.53 GHz	
GPU Memory		16 GB per GPU	
CPU Cores	8	32	64
Memory	61 GB	244 GB	488 GB
GPUs	1	4	8

Table 1: System configuration used to generate results.

facilitates the conditional execution within graphs as described in Section 5.3.6.

When a node fails to execute due to unmet dependencies, it is pushed back onto the queue of the worker which tried to execute it, which is cheap due to there being no contention with other threads for pushing and popping onto the one side of the work stealing deque. This allows other nodes to execute the node work if the dependencies are met while the node is stealing from other threads. When a node attempts to steal from other nodes, there are a number of strategies which can be used, and any number of attempts can be made before giving up and going back to a node’s own queues. Three stealing strategies are: the random strategy which randomly chooses a queue from another thread, the round robin strategy which chooses a queue by increasing index starting from one more than the stealing thread’s index, wrapping around, the topological strategy which chooses a queue based on the cache sharing properties of the thread, trying to choose queues from threads which share caches. Currently, we employ both the random and round robin strategies, however, we have seen that the performance of round robin is far superior to random stealing, likely due to the lower likelihood of two threads trying to steal from the same queue, leading to less contention. The stealing algorithm is shown in Algorithm 4.

For a node whose work needs to be executed on the GPU, it is important that the resulting graph is efficient, i.e. not introducing points where the GPU is unnecessarily idle because of over synchronization. Thus, when calling the CUDA API we use the asynchronous version of all memory related functions to ensure that threads are not blocked, and rely on atomic operations in the work stealing deque and node execution function to ensuring scheduling dependencies. Lastly, we introduce stream synchronization when a graph node requires that GPU work completes before executing the node. We use multiple streams per GPU for copy and compute to allow memory transfer and kernel execution to happen asynchronously where it is possible (for example `concurrent_padded_access()`), but place operations onto the same compute stream when it is not, since operations on the same stream are performed synchronously in the order in which they are submitted. This produces compact GPU pipelines, resulting in low overall overhead and good scaling performance, as illustrated in the results section.

Size	cuBLAS	Kokkos	Ripple	Ripple NBC
1M	0.0749	0.0421	0.0327	0.0291
10M	0.2316	0.2722	0.1704	0.1119
100M	1.5286	2.5773	1.5242	1.4622
200M	2.9785	5.1334	3.0356	2.9088
500M	7.3153	12.826	7.5261	7.2347
1B	14.556	25.618	15.048	14.439

Table 2: Results of the SAXPY computation. The Ripple NBC column is the performance using Ripple without checking the boundary condition. All times are in milliseconds.

7. Fine-grained Performance Evaluation

The performance tests in this section are all performed on a single GPU to allow a comparison against implementations of similar kernels using other frameworks or libraries designed for fine-grained parallelism, such as Kokkos [7]. The hardware configurations of the AWS compute nodes are shown in Table 1, where we use the p3.2xlarge node for single GPU tests, and all larger node types for the scaling tests in Section 8.

When implementing the kernels in Kokkos we follow the examples presented in [7], as well as the examples in the Kokkos repository. The implementations of the kernel function objects and structs for Kokkos and Ripple are very similar, with the exception that for Ripple there is a template parameter for the layout kind for any struct which is used in a benchmark.

7.1. SAXPY

The first benchmark is SAXPY which computes

$$\mathbf{y} = a * \mathbf{x} + \mathbf{y}$$

Its minimal computational requirements make it a good example for determining the overhead of the iterator functionality provided by Ripple. We compare the performance of Ripple against both cuBLAS [1] and Kokkos, with the timings shown in Table 2. For 1 billion vector elements, Ripple takes 56% of the time taken by Kokkos, and 99.2% of that taken by cuBLAS.

Profiling indicates that Ripple has a small amount of overhead for the iterator abstractions, due to the checking of the validity of the iterator. The overhead is in the range of 3-4%, but this is for a simple kernel which loads data into registers, performs a single fused multiply-add (FMA), and loads the data back to global memory. This kernel uses a one dimensional iterator, so the boundary check is only performed once. For higher dimensional data spaces the overhead would be higher, since the validity of the iterator needs to be checked for each dimension. For workloads which are more computationally intensive, however, the overhead would be a smaller relative percentage.

7.2. Particle Update in Three Dimensions

This kernel computes

$$\mathbf{x} = \mathbf{x} + \mathbf{v}\Delta t$$

where \mathbf{x} and \mathbf{v} are the three-dimensional position and velocity for each particle. This benchmark is similar to the SAXPY

Size	Kokkos	Ripple (s)	Ripple (c)	Ripple (ss)	Ripple (cs)
100k	0.0255	0.0191	0.0259	0.0221	0.0379
1M	0.1444	0.1036	0.1620	0.1343	0.2381
10M	1.2743	0.8679	1.4472	1.1834	2.0507
20M	2.5612	1.7146	2.8487	2.3441	4.0743
40M	5.0522	3.4062	5.7184	4.6741	8.1453
80M	10.112	6.7914	11.452	9.3259	16.3081

Table 3: Results of the particle update kernel for a single update for the various layouts in Ripple and for Kokkos. All times are in milliseconds. s = strided layout, c = contiguous layout, ss = strided layout in shared memory, cs = contiguous layout in shared memory.

benchmark, but requires significantly more data, which better tests the memory access performance of Ripple. Additionally, the position and velocity data require vector data types with multiple components, which can either be stored contiguously or strided.

For a three-dimensional update, the position and velocity require 12 or 24 bytes each, for single and double precision, respectively. We define a `Particle` class similar to the `State` class shown in Listing 2, to hold the particle position and velocity and use an `update(dt)` method to update the position given Δt . The results are shown in Table 3. This benchmark is memory bound, since for both the position and the velocity, each thread needs to read the six elements, perform an FMA to update the position for each dimension, and then write the results back to global memory. For contiguous data, coalesced access is not possible, so more than a single memory transaction is required per element in each vector. However, when the data is strided, only a single memory transaction is required per element so the memory access is coalesced for each element, which for this benchmark results in a 33% improvement over the contiguously laid out implementation in Kokkos, and a 40% improvement over the contiguous implementation in Ripple.

We also see that using shared memory is slower for this benchmark, due to the increase in the instruction count of the kernel. For compute architectures prior to Ampere (such as the Volta architecture used here), loading data into shared memory goes through the register file, both increasing register usage, which may reduce occupancy, as well as increasing the overall instruction count of the kernel. For a kernel with such a simple computation it is not necessary to use shared memory, since accessing data from global memory already puts the data into a register, so a load to and from shared memory reduces the performance. For the recent Ampere architecture, however, there is new functionality for copying data from global memory to shared memory asynchronously which bypasses the load into a register. This could improve performance of the shared memory results presented here. There is also more fine-grained control of the synchronization for this type of asynchronous data loading, which allows the compute cores to be utilised while waiting for the load to complete. We intend to investigate how to take advantage of this for our iterator abstractions.

7.3. Flux Difference in Two Dimensions

This benchmark computes the flux difference across all faces in two dimensions. It is a typical stencil-type computation

Size ²	Kokkos	Ripple (s)	Ripple (c)	Ripple (ss)
1k	0.2476	0.0757	0.1065	0.0921
2k	0.8259	0.2438	0.3614	0.2979
4k	3.2481	0.9101	1.3971	1.1425
8k	12.919	3.5533	5.5284	4.4941
16k	51.857	14.282	22.081	18.090
32k	215.56	59.028	86.756	74.797

Table 4: Results of a single computation of the flux difference in two dimensions for the various layouts in Ripple and for Kokkos. All times are in milliseconds. s = strided layout, c = contiguous layout, ss = strided layout in shared memory, cs = contiguous layout in shared memory.

which is used in finite volume and finite element methods. It has a larger computational component and also uses data from neighbouring cells in both dimensions. The memory access pattern is therefore more demanding than the previous benchmarks, and the kernel requires more registers for the computation. The kernel for the benchmark computes

$$\mathbf{F} = \sum_i^D F_{i+\frac{1}{2}} - F_{i-\frac{1}{2}}$$

where D is the number of dimensions, $F_{i\pm\frac{1}{2}}$ is the flux at each face of the cell in the dimension i , which can be computed with any number of methods. We choose to use the FORCE method of Toro [22]. Each cell stores a `State` data type for the solution of the Euler equations, with components for density, energy, and the velocity in each dimension. The complexity of the computation comes from the significant number of multiplications of each of the components in the `State`, which are essentially vector multiplies. The computation of the flux for the state also needs to be computed in the FORCE method, which requires evaluating the pressure from the other state variables, resulting in many reads and writes to the state data variables. As this is a two-dimensional test, the FORCE evaluation must be performed for all four faces of each cell. Lastly, padding data must be added to the domain so that the FORCE method, which requires the data from neighbouring cells in the dimension being solved, computes valid results for the first and last cell in both dimensions. Despite the additional computational complexity, the effects of data layout are the same as in the previous benchmarks, with strided data giving significantly better performance. The results are shown in Table 4. We see that on a large problem Ripple with the strided layout is 3.65 times faster than Kokkos.

7.4. Eikonal Equation Solution

The previous benchmarks, while having increasing levels of computational complexity, were all memory bound. This benchmark is computationally bound. The Eikonal equation is a special case of the nonlinear Hamilton–Jacobi partial differential equations (PDEs), defined on a Cartesian grid with a scalar speed function as

$$H(\mathbf{x}, \nabla\phi) = |\nabla\phi(\mathbf{x})|^2 - \frac{1}{f(\mathbf{x})^2} = 0$$

where $\phi(\mathbf{x})$ is a scalar field defined at each cell in the domain with location \mathbf{x} , and $f(\mathbf{x})$ the speed at the cell \mathbf{x} . Uses of the

Size ²	Kokkos	Ripple (s)	Ripple (c)	Ripple (ss)	Ripple (cs)
		float, 5 cells			
1k	0.0991	0.0712	0.1061	0.0592	0.0689
2k	0.3375	0.2294	0.3776	0.1835	0.2161
4k	1.2554	0.8720	1.4409	0.6788	0.8041
8k	5.1286	3.4141	5.7242	2.6383	3.1509
16k	20.501	13.537	22.735	10.524	12.550
	double, 10 cells				
1k	0.3150	0.1509	0.3235	0.1239	0.1756
2k	1.1978	0.5374	1.2181	0.4300	0.6341
4k	4.7241	2.0738	4.7533	1.6370	2.4578
8k	18.9335	8.1661	18.590	6.4601	9.7172
16k	76.112	32.405	73.924	25.632	38.812

Table 5: Results of the FIM solve for Ripple and for Kokkos. All times are in milliseconds. s = strided layout, c = contiguous layout, ss = strided layout in shared memory, cs = contiguous layout in shared memory.

solution of the Eikonal equation include reinitializing a level-set function and performing multi-dimensional extrapolation of data. For this benchmark we set $f(\mathbf{x}) = 1$, which is the case for reinitializing a signed-distance function.

The solution of the equation propagates information from source nodes throughout the domain—for example, for levelset reinitialization the source nodes would be the locations at which the levelset value is zero. Again, there are a number of methods which can be used to solve the Eikonal equation, such as The Fast Marching Method [23], the Fast Sweeping Method [24], [25] and the Fast Iterative Method [26] have been used for parallel implementations. We choose to use the Fast Iterative Method for this benchmark, and set a single source node at the centre of the domain. Varying the number of cells in the reinitialization band varies the computational expense of the problem, and we therefore perform the computation with different numbers of cells in the band around the source node, as well as for different levels of precision. The results are shown in Table 5. With strided layout in shared memory, Ripple is 1.95 times faster than Kokkos for 5 cells in single precision, and 2.97 times faster for 10 cells in double precision.

Using shared memory gives up to 30% improvement in performance compared to global when using strided data, while compared to contiguous data the strided shared memory improvement is closer to 90%. This difference comes from the fact that the computational component of the results contributes essentially the same time when using shared memory, regardless of data layout, however, the transfer between global and shared memory is significantly faster for strided data, as shown previously. The combination of strided data layout and shared memory gives a speedup of 2.2x and 2.88x when compared to non-shared contiguous data for float and double precision, respectively. When CUDA experience is limited, contiguous, non-shared data would typically be used, and given that the changes required by Ripple compared to such an implementation are only a few lines of code, the performance increase is significant.

```
Tensor<State, 2> in({1, 4}, padding, sizex, sizey);
Tensor<State, 2> out({1, 4}, padding, sizex, sizey);
Tensor<double, 2> wavespeeds({1, 4}, sizex, sizey);
ReductionResult<double> max_wavespeed;

Graph solve_graph;
solve_graph
  .split(set_wavespeeds, in, wavespeeds)
  .then_reduce(wavespeeds, max_wavespeed, MaxReducer)
  .then(set_dt, max_wavespeed)
  .then_split(set_boundary, in)
  .then_split(
    update_state_x, concurrent_padded_access(in), out)
  .then_split(set_boundary, out)
  .then_split(
    update_state_y, concurrent_padded_access(out), in)
  .then(swap_in_out, in, out);
```

Listing 12 Simplified Euler solver graph creation.

8. Scaling Performance

Ideally, performance of Ripple would scale linearly with an increase in computational resources, however, with multiple GPUs additional data transfer is required which introduces synchronization points, reducing the effectiveness of the parallelism. The benchmarks in this section are designed to determine the effectiveness of the framework to hide these costs. As a benchmark, we choose a solver for the 2D Euler equations since it requires many of the features of the framework described previously and will form the basis of a future application paper.

The specific problem we choose is a Mach 3.81 shock wave impacting a low density air bubble. This is a problem often used to validate a solver in computational fluid dynamics, so provides a good example of how Ripple can be used to simplify the implementation of a real-world problem. A high-level example of the code used to construct the graph which represents the Euler solver is shown in Listing 12, while the initial conditions of the problem are shown in Figure 11. For all benchmarks we run the simulation for 1000 time steps.

We also provide the efficiency of Ripple for both the strong and weak scaling cases, which quantify the percentage overhead that is added for each configuration. For weak scaling, the efficiency is computed as

$$\text{Weak Scaling Efficiency}(\%) = \frac{t_1}{t_N} * 100$$

and for strong scaling as

$$\text{Strong Scaling Efficiency}(\%) = \frac{t_1}{N * t_N} * 100$$

where for both cases, t_1 is the execution time for a single GPU, N is the number of GPUs, and t_N is the execution time for N GPUs.

8.1. Weak Scaling

We assign each GPU a partition of the domain, defined by splitting the domain in the y dimension. Each GPU requires padding data in the y dimension from either its neighbour(s) or the domain boundary, as well as padding data in the x dimension for the domain boundary data. We increase the problem

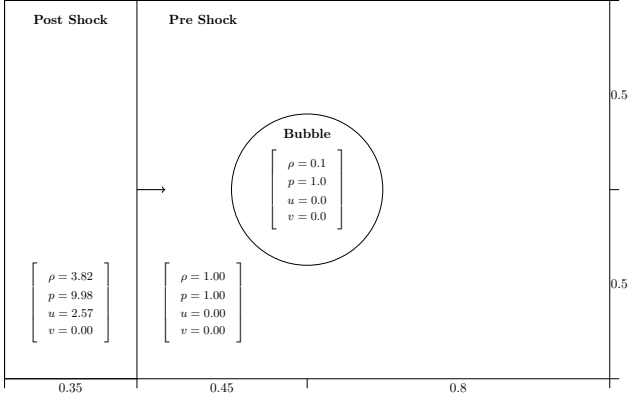


Figure 11: Initial conditions for the 2D shock bubble problem.

size in both the x and y dimensions when increasing the number of GPUs such that the problem configuration is the same relative to the domain. When more GPUs are used, the overall problem size increases, however, each GPU always has the same number of cells assigned to it, which we set to 6.4 million. The results are shown in Figure 13a, with the efficiency shown in Figure 12. Ripple performs well in the weak scaling benchmarks, introducing only a small amount of overhead and allowing a very similar computation time for a single GPU compared to 8 GPUs, as the problem size scales.

8.2. Strong Scaling

Again we assign each GPU a partition of the domain and split along the y dimension. For this benchmark we keep the problem size fixed and use two problem sizes at resolutions of 6400 by 4000 cells (small), for a total of 25.6 million cells, and 9600 by 6000 cells (large), for a total of 57.6 million cells. Adding GPUs thus decreases the number of cells on which each GPU performs computation. For perfect scaling we would expect an increase in speedup which is linear in the number of GPUs. However, since as the number of GPUs increases the relative cost of the overhead for data transfer, synchronization, and contention in the work stealing algorithm also increases, linear scaling is not practically achievable.

The results are shown in Figure 13b, with the efficiency shown in Figure 12. We achieve an increase of 6.92x for 8 GPUs at an efficiency of 87.5% for the small problem, and 7.32x at an efficiency of 91.5% for the large problem. We see that for the small problem, the cost of the overhead is high due to the small problem size, while for the larger problem the overhead is minimal since each GPU still has enough work to better hide communication costs. A significant portion of this reduction comes from the NUMA configuration of the node. When the GPUs are connected via NVLINK, the padding data transfers can be performed directly between the GPUs without going through the CPU (which is the default for Ripple when possible). However, when the GPUs are split across two sockets, with 4 GPUs per socket, and half the CPU cores on each socket, there is cross socket communication between the CPUs and GPUs. While the costs of communication between sockets

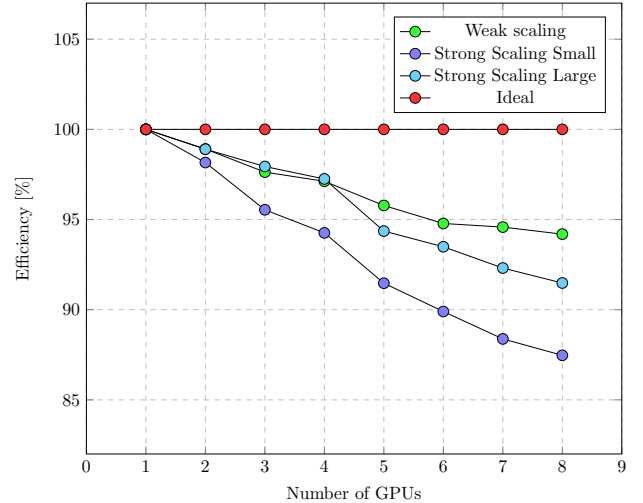


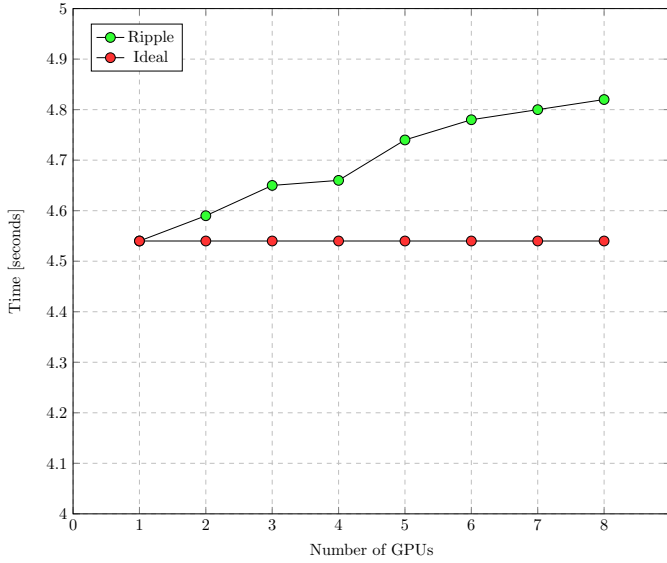
Figure 12: Scaling efficiency of Ripple for strong and weak scaling for a 2D Euler solver.

is minimal, it is still present, particularly in the work stealing algorithm which may steal tasks resulting in a CPU core submitting work to a GPU which is located on a different socket. These effects can be seen in all the scaling results, particularly in Figure 12 where the scaling between 1-4 and 5-8 GPUs have similar gradients, with a significantly larger decrease in efficiency coming from the increase from 4 to 5 GPUs. These results warrant further work into the effects of topological based algorithms for work stealing, which may reduce these effects.

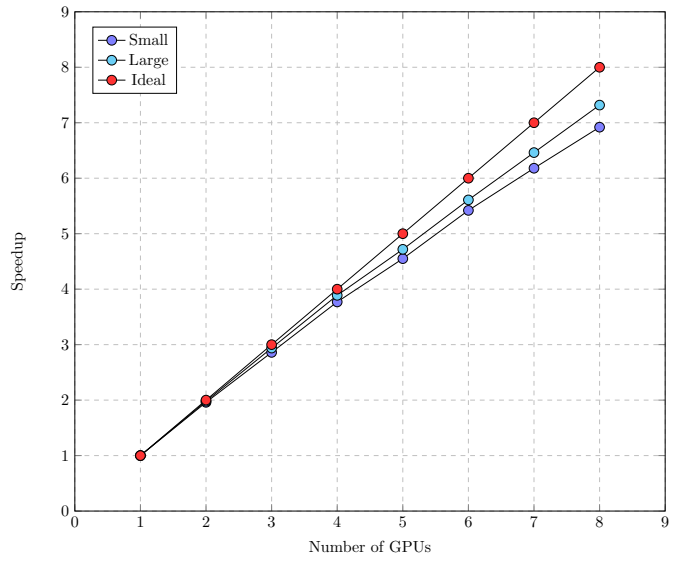
9. Limitations & Future Work

The main limitation of our library is the neighbouring region for which data can be accessed. It is only possible to access data which is on the same device as the data to which an iterator points. Therefore, if a domain is partitioned in two, one half of the domain cannot access data from the other half. However, this is true of any application which uses multiple devices, and the data would have to be sorted so that any elements which need to access each other are on the same device. Future work would add support for manipulation of the tensor data type to provide support for these kinds of use cases.

Currently, while very close to providing a unified interface for kernels which can be executed on both the CPU and the GPU, Ripple has some limitations in this area. The first is in kernels which require synchronization of threads on the GPU, through `__syncthreads()`, or our abstraction `ripple::syncthreads()`. On the CPU, this would require that a thread executes part of a function until the `syncthreads` call, saves the state for the thread, does the same for all other threads, and then resumes back at the first thread after restoring the state. This is challenging in C++; however, with the recent introduction of coroutines, it is possible to suspend a function which can later be resumed, and one area of future work is to provide this support so that there is a unified interface for both the CPU and the GPU. This would also be a starting point for



(a) Weak scaling results for Ripple across multiple GPUs.



(b) Strong scaling results for Ripple across multiple GPUs.

Figure 13: Scaling results for Ripple for a 2D Euler solver on a shock bubble problem.

allowing kernels which can be split across GPUs and CPUs, executing simultaneously, when a sufficient number of CPU cores are present.

As mentioned in Section 7.2, NVIDIA’s latest Ampere architecture allows for asynchronous data transfer between global and shared memory, with a more fine-grained synchronization model. We intend to use this to improve the performance of our library for shared memory, specifically to reduce the overhead of checking the validity of the iterators.

Improving the functionality of the allocators and the ability to create hierarchical tensor structures is another area of future work. Many applications have regions of interest within a domain which are distributed sparsely within the global computational domain, requiring adaptive, hierarchical data structures. For optimal performance on the GPU, we have shown that memory access patterns play a large role, and thus it would be ideal to allow the same access patterns but have adaptive resolution. Our tensor data structure and iterator abstractions could be extended to provide such functionality for other data types such as k-d trees, octrees, adaptive meshes, and bounding volume hierarchies, for example.

Lastly, our library is designed for single nodes with multiple GPUs and CPUs. While modern compute nodes allow for many GPUs and hundreds of CPU cores with hundreds of GB of RAM for both the CPU and GPU, some problems require still larger computational resources, and thus we could extend our library to allow for computation across any number of nodes.

10. Conclusion

We have presented the abstractions and details of our library, Ripple. Our main contributions are the ability for user-defined types to have polymorphic layouts to achieve the best possible performance on GPU accelerators, a multi-dimensional tensor

data type and iterator classes over the multi-dimensional space, a graph interface for specifying the structure of a computation, and an efficient scheduler for execution of the computational graph. Lastly, our interface allows computations to scale across all accelerators on a node, allowing high-performance computations over very large domains to be implemented with minimal programmer effort.

We have used micro benchmarks to illustrate the effectiveness of data layout polymorphism as well as the importance of utilising different physical memory spaces available in GPU accelerators. We also show how all these options are problem dependent, and that our library exposes these through simple interfaces which allow for rapid testing of the different possible configurations.

Results have been presented for strong and weak scaling cases to illustrate the effectiveness of our library on real world problems, as well as to evaluate the overhead of the abstractions provided by the library and its performance to existing frameworks. For weak scaling we achieve around 95% for 8 GPUs, while for strong scaling we achieve performance scaling of between 6.9 and 7.3x for 8 GPUs, for a common problem from computational fluid dynamics.

Ripple is under constant development and we plan to further investigate additional data structures, scheduling algorithms, and allowing our tensor data type to increase resolution in sub-regions, dynamically, for applications where computation is concentrated in certain regions. We also intend to extend the CPU interface to allow CUDA constructs such as `__syncthreads()` to work in both computational spaces, and lastly to scale to multiple nodes to allow even larger problems with minimal knowledge of parallel and distributed systems.

References

- [1] NVIDIA, CUDA toolkit documentation, 2020. URL: <https://docs.nvidia.com/cuda/index.html>.
- [2] The Khronos SYCL Working Group, Sycl 2020 specification (revision 2), 2021. URL: <https://www.khronos.org/registry/SYCL/specs/sycl-2020/pdf/sycl-2020.pdf>.
- [3] OpenMP Architecture Review Board, OpenMP Application Programming Interface, 5.0 ed., 2018.
- [4] OpenACC-Standard.org, The OpenACCC Application Programming Interface, 3.0 ed., 2019.
- [5] BSC Programming Models, OmpSs Specification, 2019.
- [6] S. Lee, J. S. Vetter, Early evaluation of directive-based GPU programming models for productive exascale computing, in: SC '12: Proceedings of the International Conference on High Performance Computing, Networking, Storage and Analysis, 2012, pp. 1–11.
- [7] H. C. Edwards, C. R. Trott, D. Sunderland, Kokkos: Enabling manycore performance portability through polymorphic memory access patterns, *Journal of Parallel and Distributed Computing* 74 (2014) 3202–3216. doi:<https://doi.org/10.1016/j.jpdc.2014.07.003>, domain-Specific Languages and High-Level Frameworks for High-Performance Computing.
- [8] C. Augonnet, S. Thibault, R. Namyst, P.-A. Wacrenier, Starpu: a unified platform for task scheduling on heterogeneous multicore architectures, *Concurrency and Computation: Practice and Experience* 23 (2011) 187–198. doi:10.1002/cpe.1631.
- [9] H. Kaiser, T. Heller, B. Adelstein-Lelbach, A. Serio, D. Fey, Hpx: A task based programming model in a global address space, in: Proceedings of the 8th International Conference on Partitioned Global Address Space Programming Models, PGAS '14, Association for Computing Machinery, New York, NY, USA, 2014. doi:10.1145/2676870.2676883.
- [10] T.-W. Huang, D.-L. Lin, Y. Lin, C.-X. Lin, Cpp-taskflow v2: A general-purpose parallel and heterogeneous task programming system at scale, 2020. [arXiv:2004.10908](https://arxiv.org/abs/2004.10908).
- [11] M. E. Belviranli, F. Khorasani, L. N. Bhuyan, R. Gupta, Cumas: Data transfer aware multi-application scheduling for shared gpus, in: Proceedings of the 2016 International Conference on Supercomputing, ICS '16, Association for Computing Machinery, New York, NY, USA, 2016. URL: <https://doi.org/10.1145/2925426.2926271>. doi:10.1145/2925426.2926271.
- [12] B. Bastem, D. Unat, W. Zhang, A. Almgren, J. Shalf, Overlapping data transfers with computation on GPU with tiles, in: 2017 46th International Conference on Parallel Processing (ICPP), 2017, pp. 171–180.
- [13] M. Wahib, N. Maruyama, T. Aoki, Daino: A high-level framework for parallel and efficient AMR on GPUs, in: SC '16: Proceedings of the International Conference for High Performance Computing, Networking, Storage and Analysis, 2016, pp. 621–632.
- [14] J. Dean, S. Ghemawat, Mapreduce: Simplified data processing on large clusters, *Commun. ACM* 51 (2008) 107–113. doi:10.1145/1327452.1327492.
- [15] D. Leijen, W. Schulte, S. Burckhardt, The design of a task parallel library, *SIGPLAN Not.* 44 (2009) 227–242. doi:10.1145/1639949.1640106.
- [16] S. Lee, R. Eigenmann, OpenMPC: Extended OpenMP programming and tuning for GPUs, in: SC '10: Proceedings of the 2010 ACM/IEEE International Conference for High Performance Computing, Networking, Storage and Analysis, 2010, pp. 1–11. doi:10.1109/SC.2010.36.
- [17] R. D. Blumofe, C. E. Leiserson, Scheduling multithreaded computations by work stealing, *J. ACM* 46 (1999) 720–748. doi:10.1145/324133.324234.
- [18] N. S. Arora, R. D. Blumofe, C. G. Plaxton, Thread scheduling for multiprogrammed multiprocessors, in: Proceedings of the Tenth Annual ACM Symposium on Parallel Algorithms and Architectures, SPAA '98, Association for Computing Machinery, New York, NY, USA, 1998, p. 119–129. doi:10.1145/277651.277678.
- [19] K. Agrawal, C. E. Leiserson, J. Sukha, Executing task graphs using work-stealing, in: 2010 IEEE International Symposium on Parallel Distributed Processing (IPDPS), 2010, pp. 1–12. doi:10.1109/IPDPS.2010.5470403.
- [20] D. Chase, Y. Lev, Dynamic circular work-stealing deque, in: Proceedings of the Seventeenth Annual ACM Symposium on Parallelism in Algorithms and Architectures, SPAA '05, Association for Computing Machinery, New York, NY, USA, 2005, p. 21–28. doi:10.1145/1073970.1073974.
- [21] N. M. Lê, A. Pop, A. Cohen, F. Zappa Nardelli, Correct and efficient work-stealing for weak memory models, *SIGPLAN Not.* 48 (2013) 69–80. doi:10.1145/2517327.2442524.
- [22] E. F. Toro, On Glimm-related schemes for conservation laws, 1996.
- [23] J. A. Sethian, A fast marching level set method for monotonically advancing fronts, *Proceedings of the National Academy of Sciences* 93 (1996) 1591–1595. doi:10.1073/pnas.93.4.1591. [arXiv:https://www.pnas.org/content/93/4/1591.full.pdf](https://www.pnas.org/content/93/4/1591.full.pdf).
- [24] H. Zhao, A fast sweeping method for eikonal equations, *Mathematics of computation* (2005).
- [25] H. Zhao, Parallel implementation of the fast sweeping method, *International Journal of Computer Mathematics - IJCM* 25 (2006).
- [26] W. Jeong, R. Whitaker, A fast iterative method for eikonal equations, *SIAM J. Sci. Comput.* 30 (2008) 2512–2534.